

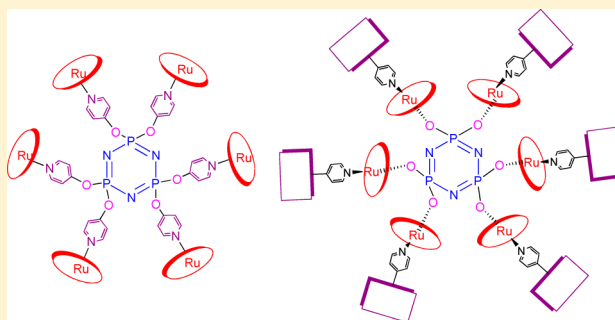
Multiporphyrin Arrays on Cyclotriphosphazene Scaffolds

Tejinder Kaur, Malakalapalli Rajeswararao, and Mangalampalli Ravikanth*

Department of Chemistry, Indian Institute of Technology Bombay, Powai, Mumbai 400 076, India

Supporting Information

ABSTRACT: We report the synthesis of first examples of hexaporphyrin and dodecaporphyrin assemblies on cyclotriphosphazene scaffold by adopting two different approaches based on Ru-pyridyl “N” coordination in decent yields. The multiporphyrin assemblies were confirmed by ^{31}P , ^{13}C , ^1H , $^1\text{H}-^1\text{H}$ COSY, and NOESY NMR spectroscopic studies. The absorption studies showed 2-fold intensity enhancement with negligible changes in peak maxima compared to porphyrin monomers. The redox potentials of multiporphyrin assemblies showed the redox features of the constituted porphyrin monomers and supported weak interactions among the porphyrin units in noncovalent hexaporphyrin and dodecaporphyrin arrays.



INTRODUCTION

Multiporphyrin arrays¹ have attracted attention to address aspects of photosynthesis, host–guest complexation, catalysis, electronic device applications, etc. Porphyrins and metalloporphyrins can be assembled into arrays either by covalent strategies or by adopting noncovalent strategies. Several covalent strategies for the synthesis of multiporphyrin arrays have evolved over the years,² but these strategies involve many sequential steps, separation of statistical mixtures, and arduous chromatographic purifications, resulting in low product yield. Noncovalent strategies³ such as hydrogen bonding, metal-mediated self-assemblies, etc. have emerged as a viable alternative to covalent synthesis in the construction of large and sophisticated multiporphyrin architectures. The mixed *meso*-substituted pyridyl/phenyl porphyrins have been used extensively to construct such multiporphyrin architectures based on self-assembly approaches using metalloporphyrin–pyridine interaction.⁴ Pyridine acts as a versatile ligand toward a variety of metal ions, and its well-known coordinating properties can be easily adopted to construct self-assembled systems. Pyridine can be functionalized easily; hence, it can be readily built into the porphyrin *meso*-position(s). Thus, the pyridyl containing compound such as *meso*-pyridyl porphyrin can act as an axial ligand to the metal atom in metalloporphyrin, provided that the metal atom inside the porphyrin core has at least one axial site available for co-ordination. Metalloporphyrins such as Zn(II), Mg(II), Ru(II), Os(II), Rh(III) porphyrins have been used to construct multiporphyrin assemblies.⁴ Recently, we showed^{5–7} that cyclotriphosphazene ring can be used as scaffold to synthesize covalent hexaporphyrin assemblies⁶ (Chart 1) under very mild reaction conditions. The hexaporphyrin assemblies on cyclotriphosphazene ring are quite stable and freely soluble in common organic solvents. These compounds can readily undergo metalation to synthesize hexametalloporphyrin assemblies. However, when we extended

the same synthetic strategy to prepare covalent cyclotriphosphazenes appended with 12 porphyrin units, it resulted in a mixture of products that requires laborious chromatographic purifications. During these investigations, we realized that cyclotriphosphazenes appended with pyrazoles and pyridines have been exploited for the synthesis of metal complexes.^{8–11} Hence, based on porphyrin literature, we thought that cyclotriphosphazenes appended with pyridines may bind metalloporphyrins as an axial ligand as well as cyclotriphosphazene ring appended with metalloporphyrins, which has a free axial site, may bind *meso*-pyridyl porphyrins to construct multiporphyrin assemblies on cyclotriphosphazene scaffolds. Here, we applied the synthetic strategy based on metal–pyridine interaction to synthesize cyclotriphosphazenes appended with 6 as well as 12 porphyrin units under simple reaction conditions in good yields. The compounds are stable, freely soluble in toluene, CH_2Cl_2 , CHCl_3 , etc. and exhibited interesting spectral and electrochemical properties.

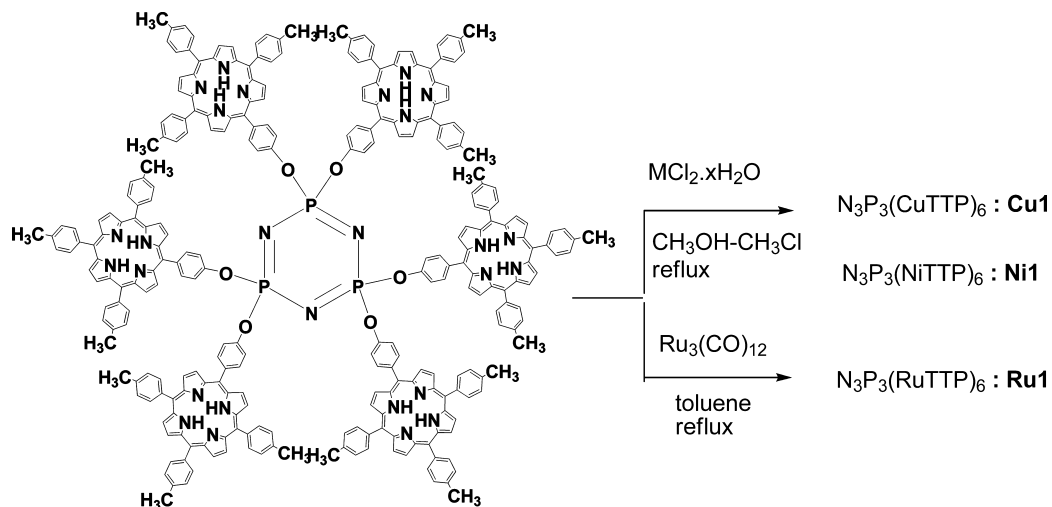
RESULTS AND DISCUSSION

Hexaporphyrin Assembly on Cyclotriphosphazene Scaffolds. The hexaporphyrin assembly on a cyclotriphosphazene scaffold (**2**) was synthesized by using the readily available cyclotriphosphazene containing 4-pyridyloxy pendant groups (**4**). (See Scheme 1.) Compound **4** was synthesized by refluxing 1 equiv of $\text{P}_3\text{N}_3\text{Cl}_6$ with 7 equiv of 4-hydroxypyridine in acetone in the presence of a base, as reported in the literature.¹² The noncovalent hexaporphyrin assembly on the cyclotriphosphazene ring **2** was synthesized by treating 1 equiv of compound **4** with 7 equiv of $\text{RuTTP}(\text{CO})(\text{EtOH})$ ¹³ in toluene at refluxing temperature for 10–12 h. The progress of the reaction was followed by TLC analysis, which clearly

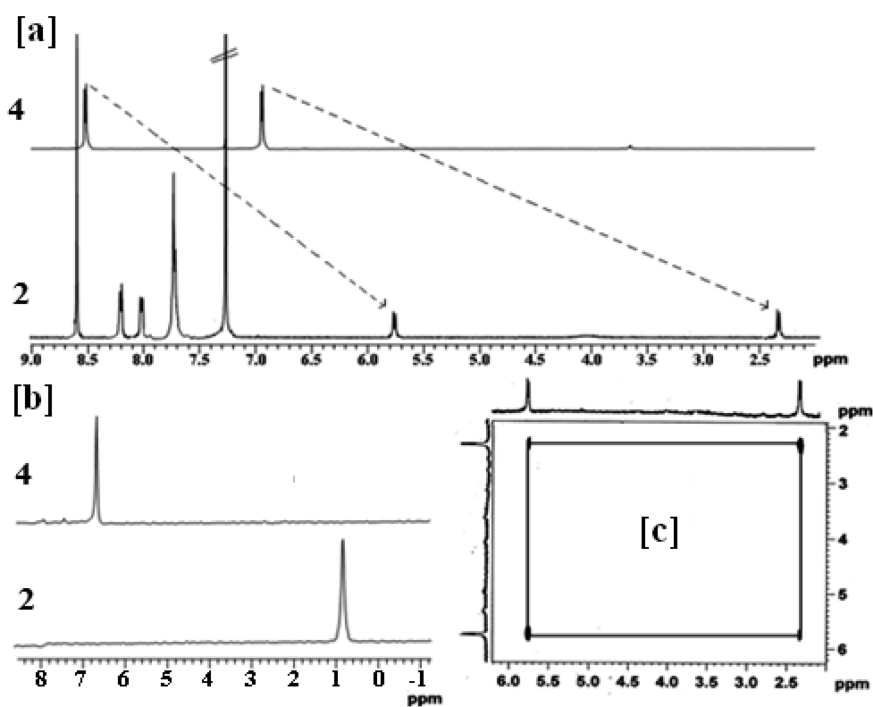
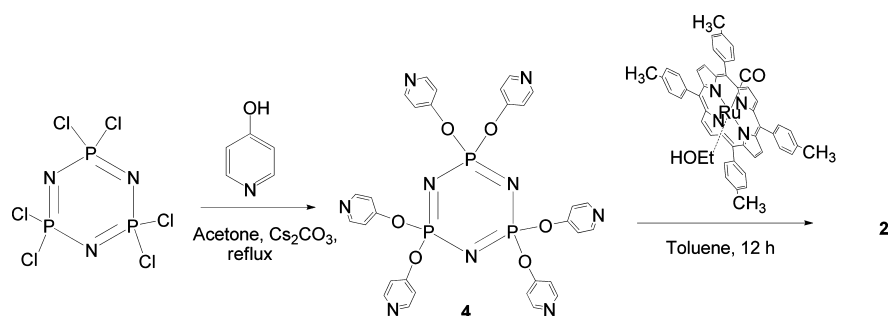
Received: July 2, 2014

Published: October 3, 2014

Chart 1. Structures of Cyclotriphosphazenes Decorated with Six Porphyrins and Their Metal(II) Derivatives



Scheme 1. Synthesis of Noncovalent Hexaporphyrin Assembly 2

Figure 1. Comparison of (a) ^1H NMR and (b) ^{31}P NMR spectra of compounds 2 and 4; (c) ^1H - ^1H -COSY NMR spectrum of 2 recorded in CDCl_3 .

indicated the spots corresponding to the formation of intermediate compounds at the beginning but as the reaction progress, those spots disappeared with an appearance of one

single spot corresponding to the required compound. The crude compound obtained after the removal of solvent was subjected to alumina column chromatographic purification and

obtained pure compound **2** as a purple solid in 69% yield. Compound **2** is sparingly soluble in common organic solvents and characterized by MALDI-TOF mass, ^1H , ^{31}P , and ^1H - ^1H COSY NMR techniques. The MALDI-TOF mass analysis did not give the molecular ion peak corresponding to compound **2**, but it did show the mass corresponding to $[\text{M}^+-6\text{RuTTP}(\text{CO})]$. The comparison of ^1H and ^{31}P NMR spectra of compounds **2** and **4** are presented in Figures 1a and 1b, respectively, along with ^1H - ^1H COSY NMR spectrum in Figure 1c. In ^1H NMR, the 3,5- and 2,6-pyridyl protons of compound **4**, which appeared as two doublets at 8.60 and 6.90 ppm, experienced a strong ring current effect upon coordination with RuTTP(CO) in compound **2** and shifted to 5.80 and 2.40 ppm, respectively. This is also clearly evident in the proton-proton connectivity pattern in the ^1H - ^1H COSY spectrum. Interestingly, unlike our earlier reported covalently linked hexaporphyrin assembly on cyclotriphosphazene ring **1** (which showed a greater number of signals for β -pyrrole and *meso*-aryl protons, which were shifted upfield, compared to monomeric porphyrin), compound **2** exhibited one singlet for pyrrole and three sets of signals for *meso*-aryl protons such as monomer RuTTP(CO)(EtOH) with no shifts in their chemical shifts. (See Figure 2.) This indicates that the

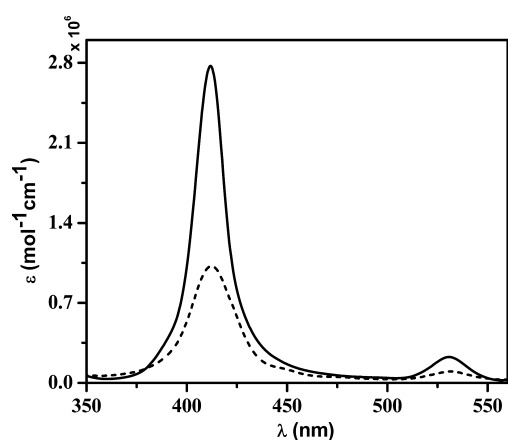
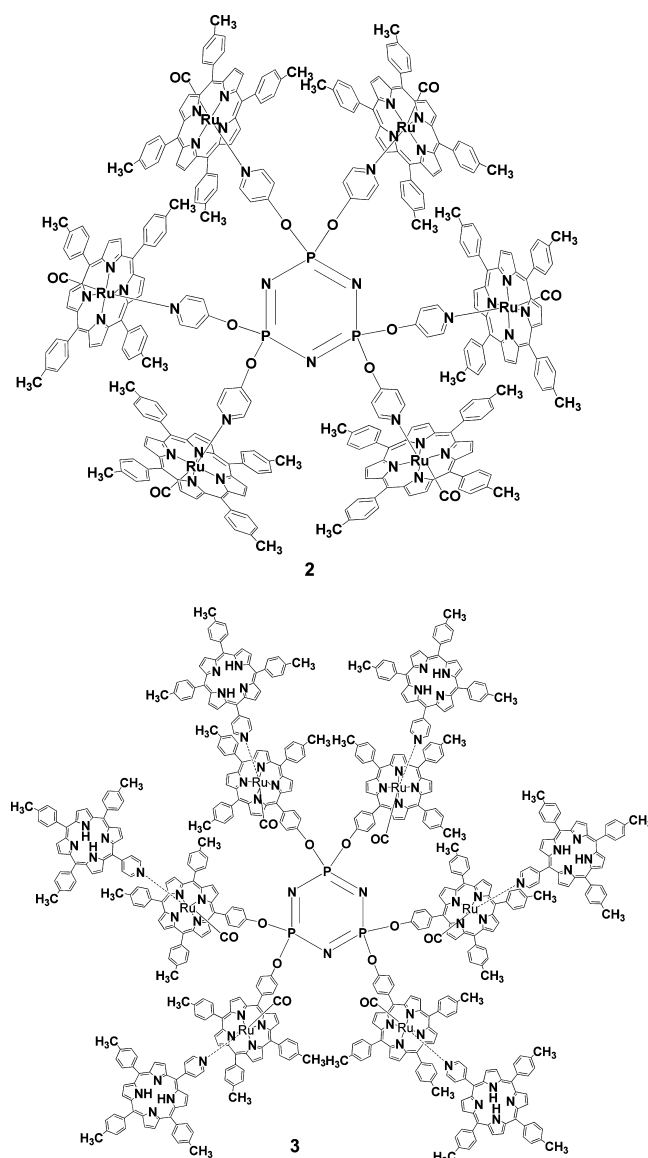


Figure 2. Comparison of (a) absorption spectra of **2** (—) and RuTTP(CO)(EtOH) (---) recorded in chloroform using concentration of 5×10^{-7} M.

strong interaction between the porphyrin units, which is present in covalent hexaporphyrin assembly **1**, is absent in noncovalent hexaporphyrin assembly **2** (see Chart 2), and Ru(II) porphyrin assembly on cyclophosphazene ring behaves as free monomeric Ru(II) porphyrin. However, the effect of RuTTP(CO) coordination to pyridyloxy units via Ru–N coordination in compound **2** was clearly reflected in the ^{31}P NMR spectrum. Compound **4** showed a signal at 6.97 ppm in ^{31}P NMR, which shifted significantly upfield in compound **2** and appeared at 0.82 ppm. This is because of the orientation of Ru(II) porphyrin, which induces the strong ring current effect on cyclotriphosphazene. This observation is in agreement with the significant upfield shifts of 2,6- and 3,5-pyridyl protons upon coordination of pyridyl “N” with RuTTP(CO) units in compound **2**. The absorption spectrum of compound **2** showed absorption features similar to monomeric RuTTP(CO)(EtOH) with identical peak positions but the intensity of absorption bands of **2** was increased by 2-fold, compared to RuTTP(CO)(EtOH) as observed earlier for covalently linked hexaporphyrin assembly **1**.

Chart 2. Structures of Noncovalent Hexaporphyrin and Dodecamer Assembly on a Cyclotriphosphazene Scaffold



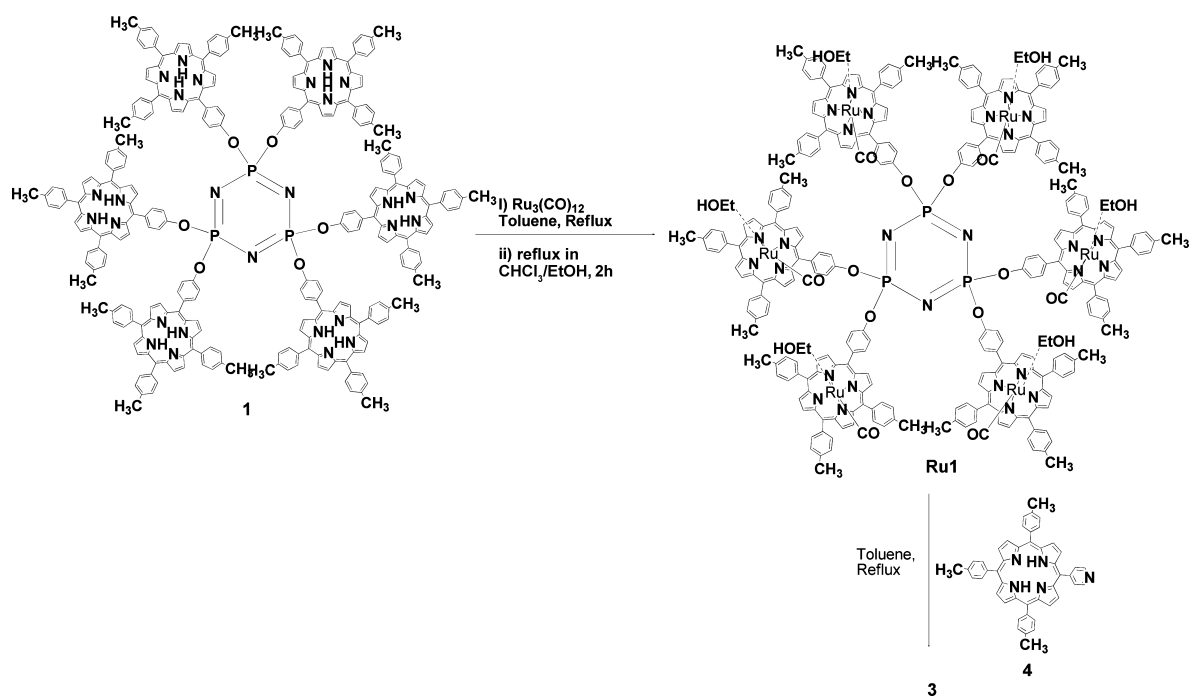
The electrochemical studies of compound **2** probed through cyclic voltammetry using tetrabutylammonium perchlorate as supporting electrolyte in dichloromethane showed two reversible oxidations and one quasi-reversible reduction (see Table 1). The peak potentials are almost in the same range as those of RuTTP(CO)(EtOH) supporting weak interaction among RuTTP(CO) units in compound **2**.

Dodecaporphyrin Assembly on a Cyclotriphosphazene Scaffold. The cyclotriphosphazene ring appended with 12 porphyrins was synthesized using **Ru1**, as shown in Scheme 2. Compound **1**⁵ was treated with $\text{Ru}_3(\text{CO})_{12}$ in toluene at reflux temperature overnight, followed by 2 h of reflux in $\text{CH}_2\text{Cl}_2/\text{EtOH}$. The progress of the reaction was followed by absorption spectroscopy. The crude compound was passed through Celite pad and afforded pure compound **Ru1** as reddish orange solid in 85% yield. **Ru1** is freely soluble in solvents such as CH_2Cl_2 , CHCl_3 , toluene, etc., and compound **Ru1** was confirmed by the molecular ion peak at 4760.7, corresponding to $[\text{M}^+-6\text{CO}]$ in MALDI-TOF mass spectrum (see the Supporting Information). ^{31}P , ^{13}C NMR, and 1D and

Table 1. Absorption and Electrochemical Data of All of the Compounds

compound	UV-Vis Data		Potential V vs SCE					
	Soret band (λ nm log ϵ)	Q bands (λ nm log ϵ)	oxidation		reduction			
2	411 (6.12)	530 (5.04) 562(sh)	1.04	1.46		-1.45		
Ru(CO)TTP	412 (5.48)	530 (4.70) 564(sh)	0.81	1.43		-1.58		
5	419 (4.71)	516 (4.52) 551 (4.33) 591 (4.22) 648 (4.15)		1.24	1.34	-0.97	-1.30	
Ru1	412 (5.48)	530 (4.70) 564(sh)	0.97		1.37		-1.39	-1.65
3	419 (6.56)	522 (5.28) 551 (5.00) 591 (4.71) 648 (4.57)	1.06	1.24	1.39	-0.99	-1.34	-1.60

Scheme 2. Synthesis of 3



2D NMR were used to characterize compound **Ru1**. In the ^{31}P NMR spectrum, **Ru1** showed only one signal at 9.88 ppm, which indicates that the **Ru1** is symmetrical and all three P atoms displayed the same chemical shift. In the ^1H NMR spectrum of **Ru1**, the signal corresponding to inner NH protons, which appears at the upfield region in free base porphyrin assembly **1** was absent, supporting that all free base porphyrin units on cyclotriphosphazene ring were metalated with Ru(II) ions. Recently, we assigned the NMR spectrum of cyclotriphosphazene appended with six free base porphyrins **1**, using 1D and 2D NMR spectroscopy. However, the comparison of ^1H NMR spectra of **Ru1** with **1** indicated that the number of signals in **Ru1** is greater compared to **1**, because of the unsymmetric nature of porphyrin upon introduction of

the Ru(II) ion. Furthermore, the signals in ^1H NMR of **Ru1** experienced slight upfield shifts, compared to **1**. Thus, it is not possible to identify all the signals in the ^1H NMR spectrum of **Ru1** based on the NMR of **1**. Hence, we carried out detailed COSY and NOESY NMR analysis of **Ru1** to identify and assign all signals in ^1H NMR spectrum. The relevant portions of COSY and NOESY NMR spectra of **Ru1** are presented in Figure 3 with detailed assignments. The ^1H NMR spectrum of **Ru1** showed few slightly broadened resonances, which we tentatively attribute to the presence of conformers in the solution. The ^1H NMR spectrum of **Ru1** showed two singlets for methyl protons at 2.67 and 2.43 ppm, corresponding to 18 and 36 protons, respectively. The signal corresponding to 18 protons at 2.67 ppm was assigned to Type I methyl protons

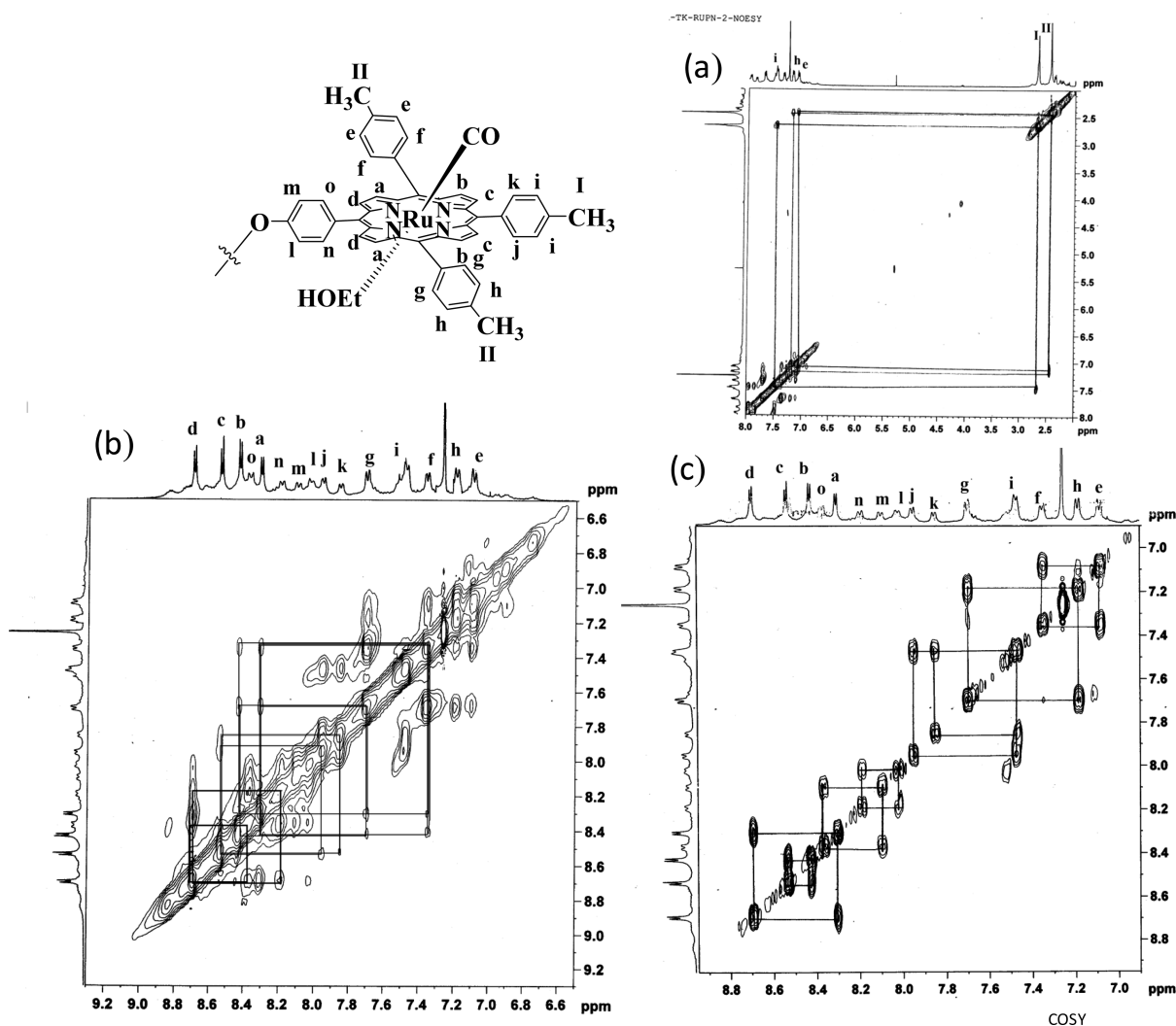


Figure 3. (a,b) Partial ^1H – ^1H COSY NMR and (c) NOESY NMR spectra of compounds **Ru1** recorded in CDCl_3 .

that are opposite to the phenoxo group, and the singlet at 2.43 ppm corresponding to 36 protons was assigned to Type II methyl protons that are *trans* to each other and reside in the same chemical environment. In the NOESY spectrum, the Type I methyl protons at 2.67 ppm showed NOE correlation with a multiplet at 7.46 ppm, which we identified as Type I protons of *meso*-aryl group. The Type I protons at 7.46 ppm show proton–proton correlation with two doublets at 7.85 and 7.96 ppm, which we assigned arbitrarily as Type k and Type j protons, respectively, of *meso*-aryl group opposite to phenoxo group. The Type k and Type j protons showed NOE correlation with a doublet at 8.54 ppm, which we assigned as Type c pyrrole protons. The doublet at 8.43 ppm was identified as being due to Type b pyrrole protons, as it showed proton–proton correlation with Type c pyrrole protons at 8.54 ppm. The Type II methyl protons at 2.43 ppm showed NOE correlation with two doublets at 7.09 and 7.18 ppm, which we assigned arbitrarily to type e and type h protons of *meso*-aryl group, respectively. The Type e protons at 7.09 ppm showed proton–proton correlation with a doublet at 7.36 ppm, which we identified as being due to Type f protons. Similarly, the Type h protons at 7.18 ppm showed NOE correlation with a doublet at 7.70 ppm, which we assigned as being due to Type g protons of the *meso*-aryl group. The Type f and Type g protons

showed NOE correlation with a doublet at 8.30 ppm, which we identified as Type a pyrrole protons. The doublet at 8.70 ppm was identified as Type d pyrrole protons, since this doublet showed proton–proton correlation with Type a protons at 8.30 ppm. The phenoxo group also showed four doublets, which were identified similarly, following NOESY and COSY correlations. The Type d pyrrole protons at 8.70 ppm showed NOE correlation with two doublets at 8.20 and 8.37 ppm, which we arbitrarily assigned as Type n and Type o protons of the phenoxo group. The Type o proton at 8.37 ppm showed proton–proton correlation with a doublet at 8.09 ppm, which we identified as Type m protons of the *meso*-phenoxo group. The Type n protons at 8.37 ppm showed proton–proton correlation with a doublet at 8.03 ppm, which we assigned as Type l protons of *meso*-phenoxo group. Thus, using 1D and 2D NMR spectroscopy, we attempted to identify all the resonances observed in the ^1H NMR spectrum of **Ru1**. Furthermore, the signal at 180 ppm in ^{13}C NMR spectrum (see the Supporting Information) confirms the presence of CO groups in compound **Ru1**. The absorption spectrum of **Ru1** showed one strong Soret band and two less-intense Q-bands. The peak positions closely matched with those of its corresponding Ru(II)porphyrin monomer RuTTP(CO)(EtOH). However, as observed for compound **1**, the absorption bands of compound

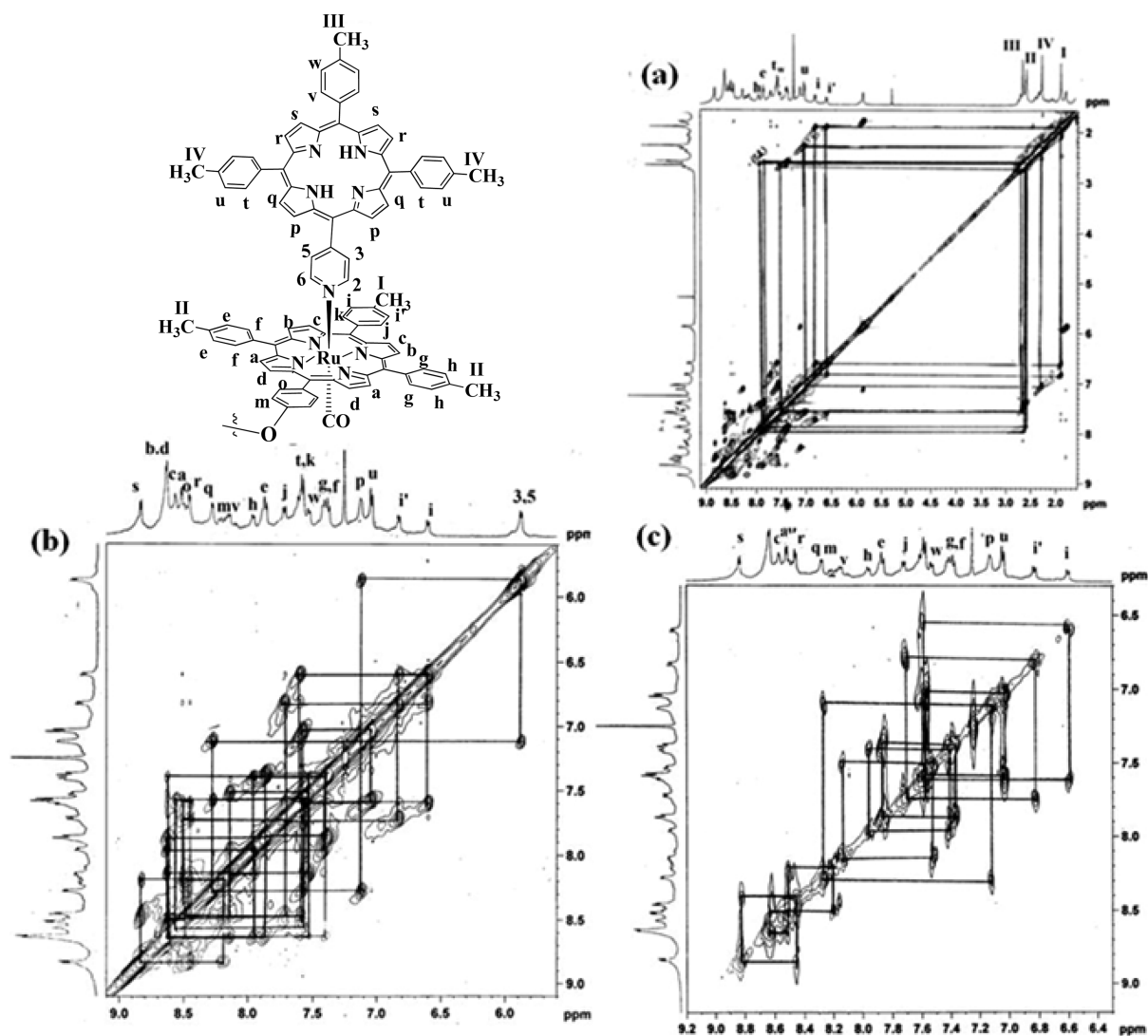


Figure 4. (a,b) Partial ^1H – ^1H COSY NMR and (c) NOESY NMR spectra of compound **2** recorded in CDCl_3 .

Ru1 are 2-fold to 3-fold more intense, with large extinction coefficients, compared to **RuTTP(CO)(EtOH)**, as presented in Table 1.

The cyclophosphazene appended with 12 porphyrins was prepared by reacting **Ru1** with 5,10,15-tri(tolyl)-20-(*p*-pyridyl) porphyrin **5** (MPy) in toluene at reflux temperature for 24 h. The crude compound was passed through Celite and afforded pure compound **3** in 88% yield after recrystallization using petroleum ether and CH_2Cl_2 . Compound **3** is soluble in toluene, CH_2Cl_2 , CHCl_3 and characterized by the MALDI-TOF mass spectrum, as well as ^{13}C ^{31}P , and 1D and 2D NMR spectroscopy. In compound **3**, the signal at 180 ppm in ^{13}C NMR spectrum and a strong sharp peak at 1943 cm^{-1} in IR spectrum corresponding to CO group of **RuTTP(CO)** is observed. In MALDI-TOF mass spectrum, a small peak at ~ 8711.8 corresponding to $[\text{M}^+ - 6\text{CO}]$ was observed along with the base peak corresponding to $[\text{M}^+ - 6(\text{CO} + \text{MPy})]$ (where M = complete molecule, MPy = monopyridyl porphyrin). This type of fragmentation is common for metal-pyridyl “N” interaction-based porphyrin arrays.³ The ^{31}P NMR spectrum of **3** showed one signal, which is shifted slightly upfield, compared to **Ru1**, supporting the symmetrical arrangement of substituents on three P atoms. The comparison of the ^1H NMR spectra of **3**,

along with its corresponding components **5** and **Ru1**, is presented in Figure 4. As clearly shown in Figure 4, the ^1H NMR spectrum of **3** is very complex and exhibit signals corresponding to Ru(II) porphyrin, as well as free base monopyridylporphyrin **5**. However, we adopted the same strategy that we used for assigning signals for **Ru1** and deduced the molecular structure of compound **3**. Similar to **Ru1**, in compound **3** also, we noted few broadened resonances in NMR spectra that could be due to the presence of conformers in solution. The COSY and NOESY NMR spectra of **3**, along with all proton assignments, are presented in Figure 4. In the NOESY spectrum of **3**, we noted four singlets at 1.90, 2.58, 2.60, 2.28 ppm, which we assigned as Type I–IV methyl protons, respectively. The Type I methyl protons of Ru(II) porphyrin units showed NOE correlation with two doublets at 6.60 and 6.83 ppm, which we arbitrarily assigned to Type i and i' protons, respectively, of the *meso* aryl group opposite to phenoxo group. The Type i and i' protons showed proton–proton correlation with a multiplet at ~ 7.58 and a doublet at ~ 7.72 ppm, which we identified as Type k and j protons, respectively. The Type k and j protons, in turn, showed NOE connectivity with a doublet at 8.51 ppm, which we identified as Type c pyrrole protons of the Ru(II) porphyrin unit. The

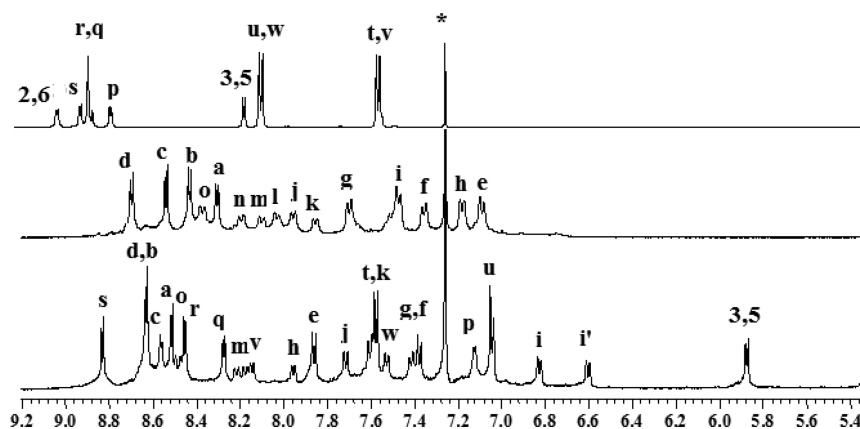


Figure 5. Comparison of ^1H NMR spectra of compound 3, along with corresponding monomers 5 and Ru1 (top to bottom).

doublet at 8.64 ppm was assigned as Type b pyrrole protons, as this doublet showed proton–proton connectivity with Type c pyrrole protons. The Type II methyl protons of Ru(II) porphyrin unit at 2.59 ppm showed NOE connectivity with two doublets at 7.86 and 7.96 ppm, which we arbitrarily assigned as Type e and h protons of Ru(II) porphyrin unit, respectively. The Type e and h protons showed proton–proton connectivity with a multiplet at 7.37–7.43 ppm, which we assigned as Type g and f protons. The Type g and f protons showed NOE connectivity with Type b, as well as with a doublet at 8.53 ppm, which we assigned as Type a pyrrole protons. The doublet at 8.64 ppm showed proton–proton connectivity with Type a pyrrole protons, which we assigned as Type d protons. Furthermore, the Type d protons showed NOE connectivity with a multiplet at ~ 8.50 ppm, which we assigned as Type o protons of the phenoxo group of Ru(II) porphyrin unit. The Type o protons, in turn, showed proton–proton connectivity with a multiplet at ~ 8.28 ppm, which we identified as being due to the Type m proton of the *meso* phenoxo group of the Ru(II) porphyrin unit.

To identify the signals corresponding to the mono *meso*-pyridyl porphyrin, we first identified the 2,6 and 3,5 protons of *meso* pyridyl group of mono *meso*-pyridyl porphyrin. The 2,6 and 3,5 *meso* pyridyl protons of monomeric *meso*-pyridyl porphyrin, which normally appears as two doublets at 9.01 and 8.18 ppm, experienced significant upfield shifts upon coordination with Ru(II) porphyrin unit via Ru(II)-pyridyl N interaction and appears at 1.81 and 5.88 ppm, respectively, in compound 3. The 2,6 and 3,5 *meso*-pyridyl protons were affected by both the inherent deshielding effect of the axial free base *meso*-pyridyl porphyrin unit and the shielding effect of the Ru(II)porphyrin unit, as detected by the proton connectivity pattern in the ^1H – ^1H COSY spectrum. The 3,5 protons at 5.88 ppm showed NOE correlation with a doublet at 7.12 ppm, which we identified as Type p pyrrole protons of *meso*-pyridyl porphyrin unit. The doublet at 8.46 ppm was assigned as Type q pyrrole protons, since this doublet showed proton–proton correlation with Type p protons. The Type IV methyl protons at 2.28 ppm showed NOE correlation with a doublet at 7.12 ppm, which we identified as Type u *meso*-aryl protons of the *meso*-pyridyl porphyrin unit. The multiplet at 7.57–7.62 ppm was identified as Type t protons as this multiplet showed COSY correlation with Type u protons. The Type t protons showed NOE connectivity with Type q protons, as well as with a doublet at 8.46 ppm, which we assigned as Type r pyrrole protons. The Type r protons further showed proton–proton

correlation with a doublet at 8.84 ppm, which we identified as Type s pyrrole protons of the *meso*-pyridyl porphyrin unit. The Type s protons showed NOE connectivity with a multiplet at ~ 7.62 ppm, which we assigned as Type v *meso*-aryl protons of the *meso*-pyridyl porphyrin unit. The Type v protons also showed ^1H – ^1H COSY correlation with Type w protons at 7.54 ppm, which, in turn, showed NOE connectivity with Type III methyl protons, which appeared as a singlet at 2.60 ppm. Furthermore, the upfield shifts noted for various protons of Ru(II) porphyrin, as well as *meso*-pyridyl porphyrin units in compound 3, were due to porphyrin ring current effect experienced by these protons.

To know more precisely about the homogeneity of compound 3, the ^1H diffusion-ordered spectroscopy (DOSY) experiments were carried out on compounds 5, Ru1, and 3 separately, as well as on a mixture containing all three compounds (5, Ru1, and 3). The DOSY experiments gives direct measure of diffusion coefficient of different compounds present in the mixture, and the diffusion coefficient is dependent on various factors, including the size and shape of the compounds. The results are displayed as a 2D spectrum in which signals are dispersed according to chemical shift in one dimension and diffusion coefficients (D) in the other. The diffusion coefficients D_{exp} obtained for compounds 5, Ru1, and 3 are 7.08, 5.37, and 3.80 ($D_{\text{exp}} = D/10^{-10} \text{ m}^2 \text{ s}^{-1}$), respectively. The diffusion coefficients are in agreement with the Stokes–Einstein equation:¹⁵ monomeric compound 5 diffuses faster, whereas dodecamer compound 3 diffuses slower, according to their relative sizes. The diffusion coefficients obtained from the mixture of compounds 5, Ru1, and 3 were in agreement with the independent compounds, suggesting that compound 3 is homogeneous. Thus, NMR studies unambiguously confirmed the structure of the porphyrin dodecamer assembly on a cyclotriphosphazene ring.

The comparison of absorption spectra of compound 3 along with its constituted porphyrin monomers monopyridyl porphyrin and RuTTP(CO)(EtOH) recorded in chloroform using same concentration is shown in Figure 5. This figure clearly shows that compound 3 exhibited absorption features of both constituted porphyrin units, and the peak maxima were almost same as those of the constituted monomers, but with a slight increase in bandwidth. Furthermore, there is a 7-fold intensity enhancement of absorption bands of compound 3, compared to its constituted porphyrin monomers.

A representative cyclic voltammogram of 3, along with those of the associated monomers, is shown in Figure 6. Generally,

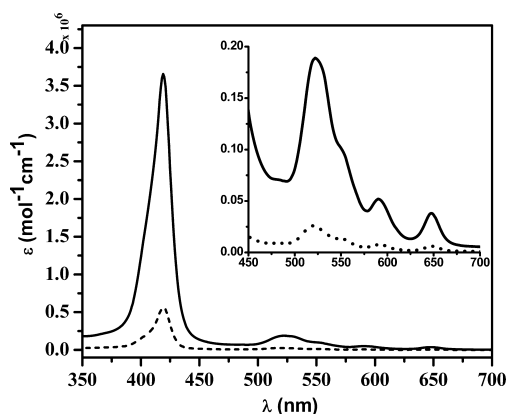


Figure 6. Comparison of absorption spectra of compound **3** and a 1:6 mixture of compounds **Ru1** and **5** recorded in chloroform using a concentration of 5×10^{-7} M.

the *meso*-pyridyl porphyrin monomers show one ill-defined oxidation due to the electron-deficient *meso*-pyridyl group but showed two quasi-reversible or reversible reductions. In compound **3**, because the *meso*-pyridyl groups are involved in binding with Ru(II), it showed three quasi-reversible oxidations and three reversible reductions. The oxidation/reduction waves were assigned by comparing with the redox properties of corresponding monomers **5** and **Ru1**. Thus, in compound **3**, the oxidation at 1.06 and 1.39 V mainly correspond to the Ru(II) porphyrin unit and oxidation at 1.24 V was mainly due to the monopyridyl porphyrin unit. Similarly, the reduction at -0.99 V corresponds to the monopyridyl porphyrin unit; the reduction at -1.34 V was due to both the monopyridyl porphyrin and Ru(II) porphyrin units, and the reduction at -1.60 V was only due to Ru(II) porphyrin unit. Since the oxidation and reduction potentials of **3** are almost in the same range as its constituted monomers, it indicated weak interaction among the porphyrin moieties in compound **3** as supported by absorption spectroscopy.

CONCLUSIONS

In summary, we used cyclotriphosphazene as a scaffold to construct two multiporphyrin assemblies such as hexaporphyrin and dodecaporphyrin assemblies by adopting two simple approaches based on Ru-pyridyl “N” coordination. The hexaporphyrin assembly is sparingly soluble but the dodecaporphyrin assembly was freely soluble in common organic solvents. The formation of multiporphyrin assemblies was confirmed by ^{31}P , ^{13}C , and 1D and 2D NMR spectroscopy. The absorption studies showed a 2-fold to 3-fold enhancement in intensity with negligible shifts in peak maxima, compared to constituted porphyrin monomers. The redox potentials of multiporphyrin assemblies are in the same range as those of porphyrin monomers. Thus, we demonstrated that the robust cyclotriphosphazene ring can be used to construct multiporphyrin assemblies by simple approaches in decent yields.

EXPERIMENTAL SECTION

All general chemicals and solvents were procured from SD Fine Chemicals, India. The known compounds such as $\text{P}_3\text{N}_3(p\text{-oxy-pyridine})_6$ (**4**),¹² covalently linked hexaporphyrin assembly on cyclotriphosphazene ring (**1**),⁵ and 5,10,15-tri(tolyl)-20-(*p*-pyridyl) porphyrin (MPy, **5**)¹⁴ were synthesized using literature methods. Column chromatography was performed using silica gel and basic alumina obtained from Sisco Research Laboratories, India. All of the

solvents used were of analytical grade and were purified and dried by routine procedures immediately before use. ^1H NMR spectra were recorded with Bruker 400 and 500 MHz instruments, using trimethylsilane (TMS) as an internal standard. All NMR measurements were carried out at room temperature in deuteriochloroform (CDCl_3). For DOSY experiment, the gradient shape was sinusoidal. The strength of the gradient shape was increased linearly, acquiring 32 gradient levels. The time between the midpoints of the gradients (Δ) was chosen as 40 ms. Low and high gradient strengths were set at 2% and 95% of maximum, respectively. All DOSY experiments were obtained with a longitudinal eddy current delay (LED) bipolar gradient pulse pair and two spoil gradients pulse sequence ledbpgp2s in the standard Bruker Pulse Sequence Library. The processing was done with standard Bruker 1D and 2D DOSY software. Absorption spectra were obtained with Varian Cary-Eclipse equipment. MALDI-TOF mass spectra were recorded on a Bruker MALDI-TOF spectrometer. Cyclic voltammetry (CV) studies carried out with BAS electrochemical system utilizing the three-electrode configuration consisting of a glassy carbon (working electrode), platinum wire (auxiliary electrode), and saturated calomel (reference electrode) electrodes in dry dichloromethane using 0.1 M tetrabutylammonium perchlorate as supporting electrolyte.

Noncovalent Hexaporphyrin Assembly (2). Compound **2** was synthesized by refluxing $\text{P}_3\text{N}_3(p\text{-oxy-pyridine})_6$ (**4**) (20 mg, 0.029 mmol) and $\text{RuTTP}(\text{CO})(\text{EtOH})$ (137 mg, 0.172 mmol), in dry toluene (20 mL) for 12 h under a nitrogen atmosphere. The solvent was evaporated under reduced pressure, and the resulted residue was subjected to basic alumina column. The desired product was eluted with petroleum ether/ CH_2Cl_2 (40:60) and was recrystallized using dichloromethane/*n*-hexane mixture to afford compound **1**. Yield: 69% (109 mg, 0.020 mmol); ^1H NMR (400 MHz, CDCl_3 , δ in ppm): δ = 2.31 (d, J = 8.0 Hz, 12H; py), 5.74 (d, J = 8.7 Hz, 12H; py), 7.71–7.72 (m, 72H; Ar), 8.02 (d, J = 8.2 Hz, 24H; Ar), 8.20 (d, J = 7.1 Hz, 24H; Ar), 8.59 (s, 48H; β -py); $^{31}\text{P}\{^1\text{H}\}$ NMR (161.8 MHz, CDCl_3 , δ in ppm): 0.82 (s). MALDI-TOF MS: m/z : Calcd (M^+) 5492.9; Found: 701.1 [M^+ -6RuTTP(CO)].

Ru1. To a solution of **1** (50 mg, 0.012 mmol) in dry toluene, $\text{Ru}_3(\text{CO})_{12}$ (77 mg, 0.120 mmol) was added and refluxed for 10 h. The color changed from purple to reddish orange as the reaction progressed. The reaction was monitored by TLC and UV-vis spectroscopy. Solvent was evaporated under vacuum, and the solid orange compound was again refluxed in dichloromethane/ethanol (1:1, 20 mL) for 2 h. After the completion of the reaction, the solvent was removed under vacuum and the resultant solid orange compound was dissolved in dichloromethane and passed through Celite. The compound was recrystallized using petroleum ether/ CH_2Cl_2 (3:1, v/v) and afforded the pure compound as reddish orange solid. Yield: 85% (53 mg, 0.010 mmol); ^1H NMR (400 MHz, CDCl_3 , δ in ppm): δ = 2.43 (s, 36H; tol), 2.66 (s, 18H; tol), 7.08 (d, J = 7.6 Hz, 12H; Ar), 7.18 (d, J = 7.2 Hz, 12H; Ar), 7.35 (d, J = 7.3 Hz, 12H; Ar), 7.47 (d, J = 7.6 Hz, 12H; Ar), 7.69 (d, J = 7.0 Hz, 12H; Ar), 7.85 (d, J = 7.2 Hz, 6H; Ar), 7.95 (d, J = 6.4 Hz, 6H; Ar), 8.04 (d, J = 7.5 Hz, 6H; Ar), 8.09 (d, J = 8.5 Hz, 6H; Ar), 8.19 (d, J = 8.4 Hz, 6H; Ar), 8.30 (d, J = 4.8 Hz, 12H; β -py), 8.38 (d, J = 8.1 Hz, 6H; Ar), 8.43 (d, J = 4.9 Hz, 12H; β -py), 8.54 (d, J = 4.9 Hz, 12H; β -py), 8.69 (d, J = 4.8 Hz, 12H; β -py); $^{31}\text{P}\{^1\text{H}\}$ NMR (161.8 MHz, CDCl_3 , δ in ppm): 9.88 (s). MALDI-TOF MS: m/z : Calcd (M^+) 4928.2; Found: 4760.7 [M^+ -6(CO)].

Noncovalent Dodecaporphyrin Assembly (3). To a solution of **1** (30 mg, 0.006 mmol) in dry toluene, 5,10,15-tri(tolyl)-20-(*p*-pyridyl) porphyrin (**5**) (23 mg, 0.035 mmol) was added and refluxed for 18 h. The reaction was monitored by TLC and UV-vis spectroscopy. After the completion of the reaction, the solvent was evaporated under vacuum and the resulted solid compound was dissolved in CH_2Cl_2 and passed through Celite. The compound was recrystallized using petroleum ether/ CH_2Cl_2 (3:1, v/v) and afforded the pure compound as a purple solid. Yield: 88% (45 mg, 0.005 mmol); ^1H NMR (500 MHz, CDCl_3 , δ in ppm): δ = -3.31 (s, 12H; $-\text{NH}$); 1.81 (d, J = 6.0 Hz, 12H, pyr), 1.90 (s, 18H; Tol), 2.28 (s, 36H; Tol), 2.59 (s, 36H; Tol), 2.66 (s, 18H; Tol), 5.87 (d, J = 6.7 Hz,

12H, pyr), 6.60 (d, $J = 7.8$ Hz, 6H, Ar), 6.83 (d, $J = 7.7$ Hz, 6H, Ar), 7.04 (d, $J = 7.8$ Hz, 24H, Ar), 7.12 (d, $J = 4.4$ Hz, 12H, β -py), 7.37–7.43 (m, 24H; Ar), 7.54 (d, $J = 8.0$ Hz, 12H, Ar), 7.57–7.62 (m, 30H; Ar), 7.72 (d, $J = 7.9$ Hz, 6H; Ar), 7.86 (d, $J = 8.0$ Hz, 12H; Ar), 7.96 (d, $J = 7.7$ Hz, 12H; Ar), 8.14–8.19 (m, 24H; Ar), 8.28 (d, $J = 4.8$ Hz, 12H; β -py), 8.46 (d, $J = 4.8$ Hz, 12H; β -py), 8.47–8.50 (m, 12H; Ar), 8.51 (d, $J = 4.7$ Hz, 12H; β -py), 8.56 (d, $J = 4.8$ Hz, 24H; β -py), 8.84 (d, $J = 4.7$ Hz, 12H; β -py); $^{31}\text{P}\{^1\text{H}\}$ NMR (161.8 MHz, CDCl_3 , δ in ppm): 9.01 (s). ^{13}C NMR (400 MHz CDCl_3): 181.0, 151.2, 144.1, 140.1, 139.4, 136.8, 135.7, 134.3, 133.6, 131.7, 127.3, 127.1, 121.9, 120.3, 32.1, 29.9, 29.5, 22.8, 21.6, 21.5, 14.3; MALDI-TOF MS: m/z : Calcd (M^+) 8881.2; Found: 8711.8 [$\text{M}^+ - (6\text{CO})$].

■ ASSOCIATED CONTENT

Supporting Information

This material is available free of charge via the Internet at <http://pubs.acs.org>.

■ AUTHOR INFORMATION

Corresponding Author

*E-mail: ravikanth@chem.iitb.ac.in.

Notes

The authors declare no competing financial interest.

■ ACKNOWLEDGMENTS

M.R. and T.K. thanks Department of Science & Technology, Government of India for funding the project. We thank Central Facility, MALDI-TOF/TOF, IIT–Bombay, for recording the MALDI-TOF mass spectra.

■ REFERENCES

- (1) (a) Nakamura, Y.; Aratani, N.; Osuka, A. *Chem. Soc. Rev.* **2007**, *36*, 831. (b) Shinokubo, H.; Osuka, A. *Chem. Commun.* **2009**, 1011. (c) Burrell, A. K.; Officer, D. L.; Plieger, P. G.; Reid, D. C. W. *Chem. Rev.* **2001**, *101*, 2751. (d) Aratani, N.; Tsuda, A.; Osuka, A. *Synlett* **2001**, *11*, 1663. (e) Kim, D.; Osuka, A. *Acc. Chem. Res.* **2004**, *37*, 735. (f) Holten, D.; Bocian, D. F.; Lindsey, J. S. *Acc. Chem. Res.* **2002**, *35*, 57. (2) (a) Wagner, R. W.; Seth, J.; Yang, S.-I.; Kim, D.; Bocian, D. F.; Holten, D.; Lindsey, J. S. *J. Org. Chem.* **1998**, *63*, 5042. (b) Ambrose, J.; Li, A.; Yang, S.-I.; Diers, J. R.; Seth, J.; Wack, C. R.; Bocian, D. F.; Holten, D.; Lindsey, J. S. *J. Am. Chem. Soc.* **1999**, *121*, 8927. (c) Song, H.-E.; Kirmaier, C.; Schwartz, J. K.; Hindin, E.; Yu, L.; Bocian, D. F.; Lindsey, J. S.; Holten, D. *J. Phys. Chem. B* **2006**, *110*, 19131. (d) Sugiura, K.; Fujimoto, Y.; Sakata, Y. *Chem. Commun.* **2000**, 1105. (e) Cho, H. S.; Rhee, H.; Song, J. K.; Min, C.-K.; Takase, M.; Aratani, N.; Cho, S.; Osuka, A.; Joo, T.; Kim, D. *J. Am. Chem. Soc.* **2003**, *125*, 5849. (f) Shoji, O.; Okada, S.; Satake, A.; Kobuke, Y. *J. Am. Chem. Soc.* **2005**, *127*, 2201. (g) Drain, C. M.; Varotto, A.; Radivojevic, I. *Chem. Rev.* **2009**, *109*, 1630. (h) Beletskaya, L.; Tyurin, V. S.; Tsivadze, A. Y.; Guillard, R.; Stern, C. *Chem. Rev.* **2009**, *109*, 1659–1713. (3) (a) Shinmori, H.; Kajiwara, T.; Osuka, A. *Tetrahedron Lett.* **2001**, *42*, 3617–3620. (b) Hunter, C. A.; Sarson, L. D. *Angew. Chem., Int. Ed. Engl.* **1994**, *33*, 2313. (c) Sessler, J. L.; Wang, B.; Harriman, A. *J. Am. Chem. Soc.* **1995**, *117*, 704. (d) Karl, V.; Springs, S. L.; Sessler, J. L. *J. Am. Chem. Soc.* **1995**, *117*, 8881. (e) Aoyama, Y.; Tanaka, Y.; Toi, H.; Ogoshi, H. *J. Am. Chem. Soc.* **1988**, *110*, 4076. (f) Anderson, H. L.; Sanders, J. K. M. *J. Chem. Soc. Chem. Commun.* **1993**, 456. (g) Chi, X.; Guerin, A. J.; Haycock, R. A.; Hunter, C. A.; Sarso, L. D. *J. Chem. Soc. Chem. Commun.* **1995**, 2567. (h) Anderson, H. L.; Sanders, J. K. M. *J. Chem. Soc. Chem. Commun.* **1989**, 1714. (i) Bonar-Law, R. P.; Mackay, L. G.; Sanders, J. K. M. *J. Chem. Soc. Chem. Commun.* **1993**, 456. (j) Drain, C. M.; Lehn, J. M. *J. Chem. Soc. Chem. Commun.* **1994**, 2313. (k) Karia, N.; Imamura, T.; Sasaki, Y. *Inorg. Chem.* **1998**, *37*, 1658. (l) Anderson, H. L.; Hunter, C. A.; Neah, M. N.; Sanders, J. K. M. *J. Am. Chem. Soc.* **1990**, *112*, 5780. (m) Harriman, A.; Sauvage, J. P. *Chem. Soc. Rev.* **1996**, *41*. (n) Collin, J. P.; Guillerez, S.; Sauvage, J. P.;

Bargellitti, F.; Cola, L. D.; Flamigni, L.; Balzani, V. *Inorg. Chem.* **1991**, *30*, 4230. (o) Harriman, A.; Odobel, F.; Sauvage, J. P. *J. Am. Chem. Soc.* **1994**, *116*, 5481. (p) Collin, J. P.; Harriman, A.; Heitz, V.; Odobel, F.; Sauvage, J. P. *J. Am. Chem. Soc.* **1994**, *116*, 5679. (q) Amabillino, D. B.; Sauvage, J. P. *New. J. Chem.* **1998**, 395. (r) Collin, J. P.; Gavina, P.; Heitz, V.; Sauvage, J. P. *Eur. J. Inorg. Chem.* **1998**, *1*, 14. (s) Flamigni, L.; Barigelletti, F.; Armaroli, N.; Ventura, B.; Collin, J. P.; Sauvage, J. P.; Williams, J. A. G. *Inorg. Chem.* **1999**, *38*, 661. (t) Noblat, S.; Dietrich-Buchecker, C. O.; Sauvage, J. P. *Tetrahedron Lett.* **1987**, *28*, 5829. (u) Solladie, N.; Chambron, J.-C.; Dietrich-Buchecker, C. O.; Sauvage, J. P. *Angew. Chem., Int. Ed. Engl.* **1996**, *35*, 906.

(4) (a) Iengo, E.; Zangrando, E.; Alessio, E. *Acc. Chem. Res.* **2006**, *39*, 841. (b) Iengo, E.; Zangrando, E.; Alessio, E. *Eur. J. Inorg. Chem.* **2003**, *13*, 2371.

(5) Rajeswara Rao, M.; Gayatri, G.; Kumar, A.; Sastry, G. N.; Ravikanth, M. *Chem.—Eur. J.* **2009**, *15*, 3488.

(6) Rajeswara Rao, M.; Ghosh, A.; Ravikanth, M. *Inorg. Chim. Acta* **2011**, *372*, 436.

(7) Pareek, Y.; Ravikanth, M. *Chem.—Eur. J.* **2012**, *18*, 8835. Rajeswara Rao, M.; Ghosh, A.; Ravikanth, M. *Inorg. Chim. Acta* **2011**, *372*, 436.

(8) Ainscough, E. W.; Brodie, A. M.; Depree, C. V. *J. Chem. Soc., Dalton Trans.* **1999**, 4123.

(9) Ainscough, E. W.; Brodie, A. M.; Depree, C. V.; Moubaraki, B.; Murray, K. S.; Otter, C. A. *Dalton Trans.* **2005**, 3337.

(10) Ainscough, E. W.; Brodie, A. M.; Depree, C. V.; Jameson, G. B.; Otter, C. A. *Inorg. Chem.* **2005**, *44*, 7325.

(11) Ainscough, E. W.; Brodie, A. M.; Depree, C. V.; Otter, C. A. *Polyhedron* **2006**, *25*, 2341.

(12) Carriedo, G. A.; Elipe, P. G.; Alonso, F. J. G.; Catuxo, L. F.; Diaz, M. R.; Granda, S. G. *J. Organomet. Chem.* **1995**, *498*, 207.

(13) Collman, J. P.; Barnes, C. E.; Brothers, P. J.; Collins, T. J.; Ozawa, T.; Gallucci, J. C.; Ibers, J. A. *J. Am. Chem. Soc.* **1984**, *106*, 5151.

(14) Shetti, V. S.; Ravikanth, M. *Inorg. Chem.* **2011**, *5*, 1713.

(15) Holz, M.; Mao, X.-a.; Seiferling, D.; Sacco, A. *J. Chem. Phys.* **1996**, *104*, 669.